(7) Dubault, A.; Casagrande, C.; Veyssie, M. *J. Phys. Chem.* **1975**, *79*, 2254-2259.
(8) Letts, S. A.; Fort Jr., T.; Lando, J. B. *J. Colloid Interface Sci.* **1976**, *56*, 64-75.
(9) Day, D. R.; Ringsdorf, H. *Makromol. Chem.* **1979**, *180*, 1059-1063.
(10) O'Brien, K. C.; Rogers, C. E.; Lando, J. B. *Thin Solid Films* **1983**, *102*, 131-140.
(11) Hupfer, B.; Ringsdorf, H. *Chem. Phys. Lipids* **1983**, *33*, 263-282.
(12) Holden, D. A.; Ringsdorf, H.; Haubs, M. *J. Am. Chem. Soc.* **1984**, *106*, 4531-4536.
(13) Elbert, R.; Laschewsky, A.; Ringsdorf, H. *J. Am. Chem. Soc.* **1985**, *107*, 4134-4141.
(14) Higashi, N.; Kunitake, T. *Chem. Lett.* (*Jpn.*) **1986**, *105*-108.
(15) Laschewsky, A.; Ringsdorf, H.; Schmidt, G.; Schneider, J. *J. Am. Chem. Soc.* **1987**, *109*, 788-796.
(16) Fendler, J. H.; Tundo, P. *Acc. Chem. Res.* **1984**, *17*, 3-7.
(17) Rolandi, R.; Flom, S. R.; Dillon, I.; Fendler, J. H. *Prog. Colloid Polym. Sci.* **1987**, *73*, 134-141. Zhao, X. K.; Baral, S.; Rolandi, R.; Fendler, J. H. *J. Am. Chem. Soc.* **1988**, *110*, 1012-1024.
(18) Reed, W.; Guterman, L.; Tundo, P.; Fendler, J. H. *J. Am. Chem. Soc.* **1984**, *106*, 1897-1907.
(19) Nome, F.; Reed, W.; Politi, M.; Tundo, P.; Fendler, J. H. *J. Am. Chem. Soc.* **1984**, *106*, 8086-8093.
(20) Serrano, J.; Mucino, S.; Millan, S.; Reynoso, R.; Fucugauchi, L. A.; Reed, W.; Nome, F.; Tundo, P.; Fendler, J. H. *Macromolecules* **1985**, *18*, 1999-2005.
(21) Reed, W.; Lasic, D.; Hauser, H.; Fendler, J. H. *Macromolecules* **1985**, *18*, 2005-2012.
(22) Yuan, Y.; Tundo, P.; Fendler, J. H. *Macromolecules* **1989**, *22*, 29-35.
(23) Rolandi, R.; Paradiso, R.; Xu, S. Q.; Palmer, C.; Fendler, J. H. *J. Am. Chem. Soc.*, in press.
(24) Mingins, J.; Owens, N. F. *Thin Solid Films* **1987**, *152*, 9-28.
(25) Gaines, G. L., Jr. *J. Colloid Interface Sci.* **1966**, *21*, 315-319.
(26) Goodrich, F. C. *Proc. 2nd Int. Congr. Surf. Activity I* **1951**, 85-91.
(27) Gaines, G. L. *Insoluble Monolayers at Liquid-Gas Interfaces*; Wiley: New York, 1966.
(28) Gershfeld, N. L. *Ann. Rev. Phys. Chem.* **1976**, *27*, 349-368.
(29) Joos, P. *Bull. Soc. Chim. Belges* **1969**, *78*, 207-217.
(30) Joos, P.; Demel, R. A. *Biochim. Biophys. Acta* **1969**, *183*, 447-457.
(31) Zsako, J.; Tomoaia-Cotisel, M.; Chifu, E. *J. Colloid Interface Sci.* **1984**, *102*, 186-205.
(32) Defay, R.; Prigogine, I.; Bellemans, A.; Evertt, D. H. *Surface Tension and Adsorption*; Longmans & Green: London, 1966.
(33) Costin, I. S.; Barnes, G. T. *J. Colloid Interface Sci.* **1975**, *51*, 106-121.
(34) Tancrède, P.; Parent, L.; Leblanc, R. M. *J. Colloid Interface Sci.* **1982**, *89*, 117-123.
(35) Robert, S.; Tancrède, P.; Salesse, C.; Leblanc, R. M. *Biochim. Biophys. Acta* **1983**, *730*, 217-225.
(36) Tancrède, P.; Munger, G.; Leblanc, R. M. *Biochim. Biophys. Acta* **1982**, *689*, 45-54.
(37) Thin-layer chromatography of polymerized vesicles prepared from 1 showed no traces of cleaved products. Presence of 1% deliberately added single-chain carboxylic acid surfactant was shown to be detectable.
(38) Flory, P. J. *Principles of Polymer Chemistry*; Cornell University Press: Ithaca, N.Y. 1953; p 111.
(39) The value of Φ_r has been determined to be 0.106.[17] The molar extinction coefficient ($\epsilon_{266\ nm}$ = 1600 M^{-1} cm^{-1}) was converted to a molecular cross section by $\epsilon_{266\ nm} = 1.6 \times 10^3$ M^{-1} cm^{-1} $L(10^3\ cm^3)/L \times 1$ mol/$(6.02 \times 10^{23}$ monomer) = 2.7×10^{-18} cm^2/monomer. Table II gives $\bar{\epsilon I}$ values ($\bar{\epsilon I}$ = integral ($\lambda_1 \rightarrow \lambda_2$) of $\bar{\epsilon I}$ dλ) values for steady-state irradiation intensities. Using a very narrow band path ($^1/_2$ half-bandwidth = 5 nm) allowed us to carry out the integration between 243 and 250 nm.

Temperature Dependence of Crystal Lattice Modulus and Dynamic Mechanical Properties of Ultradrawn Polypropylene Films

Chie Sawatari† and Masaru Matsuo*

Department of Clothing Science, Faculty of Home Economics, Nara Women's University, Nara 630, Japan. *Received May 5, 1988; Revised Manuscript Received November 29, 1988*

ABSTRACT: The temperature dependence of the crystal lattice modulus of polypropylene was measured by X-ray diffraction using ultradrawn films produced by gelation/crystallization from solutions. Measurements were carried out in the temperature range 20–160 °C for specimens with draw ratios of about 100. The measured crystal lattice modulus was in the range 40.6–41.4 GPa, and the values were independent of temperature. In contrast, the storage modulus of the films decreased with increasing temperature. This discrepancy was related to an increase in the amorphous content with increasing temperature, and this tendency became enhanced at temperatures above 130 °C. Furthermore, in terms of relative molecular orientation, the relaxation mechanism was discussed as a function of draw ratio by using master curves constructed by shifting horizontally and then vertically. Thus the Arrhenius plots of log shift factor versus reciprocal of the absolute temperature indicate that there exist two mechanical dispersions corresponding to the α and β mechanisms for drawn specimens with draw ratios >100. The values of activation energies associated with the α and β mechanisms decrease accordingly as the draw ratio increases. Incidentally, the values, 129 and 82 kJ/mol, of the α and β mechanisms for the undrawn films are lower than those reported already.

Introduction

It is well-known that molecular chains with ultradrawn films are aligned almost perfectly in the stretching direction. Such a simple morphology has the advantage of permitting an estimate of the crystal lattice modulus and the mechanical dispersion of polymeric materials.[1,2] On the basis of this concept, Matsuo et al. have studied the temperature dependence of the crystal lattice modulus[3] and the crystal dispersion[4,5] using ultradrawn polyethylene films prepared by gelation/crystallization from dilute solution by the method of Smith and Lemstra[6,7] and then were elongated in a hot oven at 135 °C. The temperature dependence of the crystal lattice modulus was measured in the temperature range 20–150 °C for the specimens with the draw ratios >300.[3] The resultant values were independent of temperature up to 145 °C (close to the theoretical melting point of 145.5 °C[8]) and were in the range 211–222 GPa. In contrast, although the storage modulus

* To whom correspondence should be addressed.
† Present address: Faculty of Education, Shizuoka University, Shizuoka 442, Japan.

0024-9297/89/2222-2968$01.50/0

of a specimen with a draw ratio of 400 reached 216 GPa at 20 °C, corresponding to the crystal lattice modulus, it decreased with increasing temperature. This difference was discussed in terms of the increase in the amorphous content with increasing temperature. This phenomenon was formulated on the basis of a model system, in which anisotropic amorphous layers lie adjacent to the oriented crystal layers with the interface perpendicular to the stretching direction.[9] Apart from this treatment, the temperature dependence of the tensile strength has been discussed at a given molecular weight by Termonia et al. using the stochastic model for failure of perfectly ordered and oriented polyethylene filaments.[10,11] The calculated result indicated a drastic decrease in the tensile strength with increasing temperature.

The difference in temperature dependence between the crystal lattice modulus and the storage modulus served to analyze the crystal dispersion in terms of relative orientation of molecular chains.[5] It turned out that two relaxations designated as the α_1 and α_2 mechanisms exhibit considerable anisotropic properties, as has been reported by Kawai et al.[12,13] The α_1 mechanical dispersion is assigned to interlamellar grain boundary phenomena associated with reorientation of crystal grains due to their own preferential rotation within the orienting crystal lamellae. The α_1 dispersion of ultradown films was related to the slippage of the crystal grains in the c-axis direction.[5] The α_2 mechanism is ascribed to a smearing-out effect of the crystal lattice potential due to the onset of rotational oscillation of polymer chains within the crystal grain. It was clearly observed when the applied external excitation is perpendicular to the c axis but it less obvious when it is parallel to the c axis.

To further understand the mechanical properties of highly oriented polymeric system, this paper explores the temperature dependence of the crystal lattice modulus as well as that of the crystal dispersion of polypropylene films prepared by gelation/crystallization from solutions[14-16] and elongated to desired draw ratios at 165–170 °C. According to a previous paper,[15] the Young's modulus of ultradrawn films with a draw ratio of 100 reached 40.4 GPa, which corresponds to a crystal lattice modulus of 41 GPa at 20 °C. This specimen is morphologically simpler than a spherulitic one, since the molecular chains are fully extended and aligned with respect to the stretching direction.

Experimental Section

Isotactic polypropylene of high molecular weight (4.4×10^6) was employed. Gel films were prepared following the method of Smith and Lemstra.[6,7] The detailed method to prepare the gels has been discussed elsewhere.[2,15] The gel films were stretched to the desired draw ratios in the temperature range 165–170 °C.

Figure 1 shows the wide-angle X-ray diffraction (WAXD) patterns and small-angle light-scattering (SALS) patterns under H_v polarization condition as a function of the draw ratio λ. The X-ray measurements were carried out with a 12-kW rotating-anode X-ray source (Rigaku RDA-rA). The WAXD patterns were observed with a flat-film camera using Cu Kα radiation at 200 mA and 40 kV. The X-ray beam was monochromatized with a curved graphite monochromator. The exposure time was 1 h. As λ increases, the WAXD patterns exhibit clear diffraction spots of the (130), (040), and (110) planes characterizing a very high orientation of the c axis with respect to the stretching direction. The SALS patterns were obtained with 3-mW He–Ne gas laser as a light source. Diffuse surfaces were avoided by sandwiching a specimen between microcover glasses with a silicone immersion oil having a refractive index of 1.556. The H_v pattern of the undrawn film displays lobes of a diffuse X type. The intensity distribution has a maximum in the center and decreases monotonically with increasing scattering angle. These observations are indicative of scattering from rodlike textures. The existence

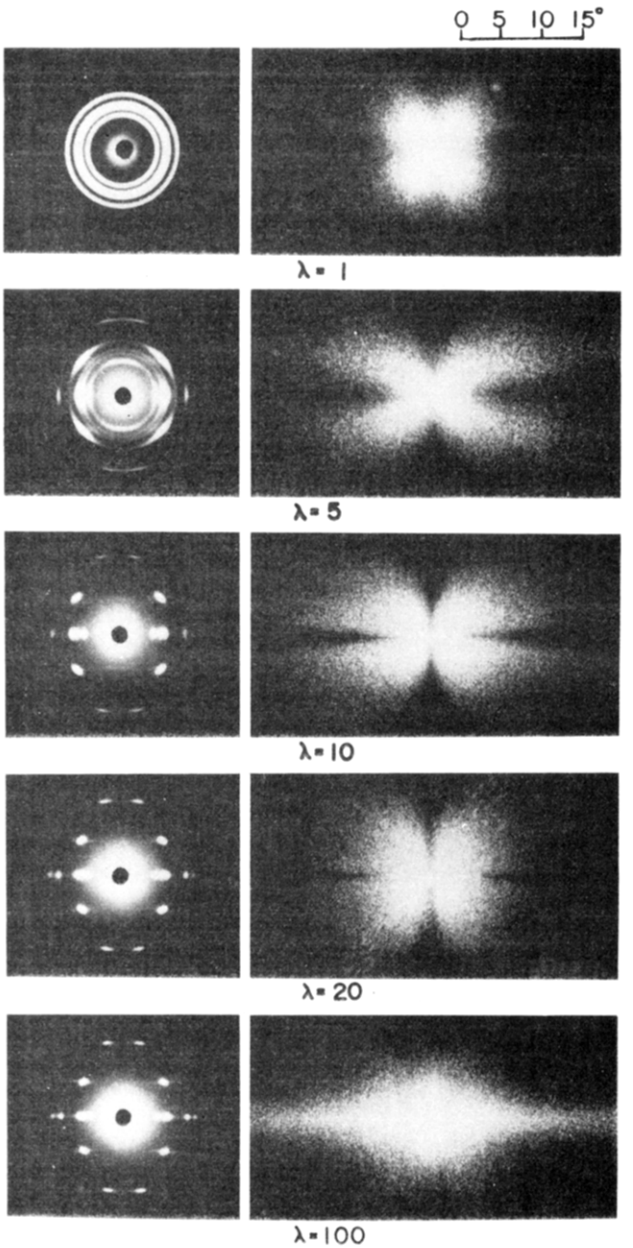

Figure 1. WAXD patterns (left hand) and SALS patterns (right hand) under H_v polarization conditions for polypropylene films with the indicated draw ratios.

Table I
Characteristics of Polypropylene Gel Films with the Indicated Draw Ratios

draw ratio (λ)	Young's modulus, GPa	tensile strength, GPa	crystallinity, %	melting point, °C
1			72.8–73.2	165
20	10.3–13.3	0.457–0.521	77.2–78.1	167
40	19.2–21.4	0.750–0.994	80.4–81.3	170
100	33.8–40.4	1.35–1.56	82.6–86.4	176–178

of rodlike textures has been observed for ultrahigh molecular weight polyethylene gel films.[17] In the initial elongation, the scattering lobes are extended in the horizontal direction. These profiles exhibit scattering characteristic of rodlike textures oriented in the stretching direction. In contrast, the scattering lobes beyond $\lambda = 20$ are extended in the vertical direction, as has been observed for the oriented crystallization of polyethylene.[17] At $\lambda = 100$, the lobes become indistinct, indicating the scattering from disruptive rods.

Table I shows the characteristics of bulk specimens with increasing draw ratio λ. The Young's modulus, tensile strength,

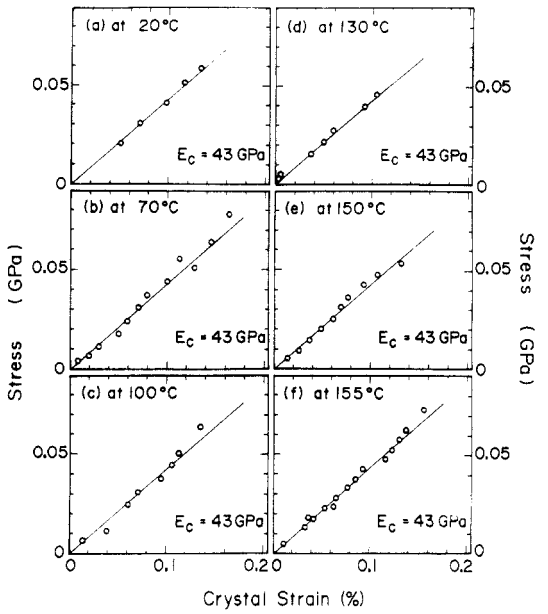

Figure 2. Temperature dependence of the crystal lattice modulus of the ($\bar{1}13$) plane up to 155 °C for drawn specimens with draw ratios >80.

crystallinity, and melting point increase as λ increases. They attain their maximum values when the draw ratio reaches 100.

As discussed in a previous work,[2] the crystal lattice modulus of polypropylene cannot be observed directly since there exists no detectable crystal plane whose reciprocal lattice vector is parallel to the crystal chain axis. In the unit cell of polypropylene, the reciprocal lattice vector of the ($\bar{1}13$) plane, among all the crystal planes, most closely parallels the c axis. Hence, the apparent crystal modulus of the ($\bar{1}13$) plane was measured, and subsequently the real value of the crystal lattice modulus was derived from the apparent modulus by a somewhat complicated mathematical treatment.[2]

To measure the crystal lattice modulus exactly, great care was taken to avoid further elongation of the drawn test specimen under the external applied stress at temperatures above 130 °C. Further elongation under constant stress, termed "creep", is associated with viscoelastic properties and invalidates the homogeneous stress hypothesis. The creep phenomenon was negligible when specimens drawn beyond $\lambda = 80$ were annealed for 1 h at 150 °C and cooled slowly to room temperatures at a constant stress of 24.5 MPa prior to measurement of the crystal lattice strain.

The complex dynamic tensile modulus was measured at frequencies from 0.1 to 100 Hz over the temperature range 20–120 °C by using a viscoelastic spectrometer (VES-F) obtained from Iwamoto Machine Co. Ltd. to study the crystal dispersion. The length of the specimen between the jaws was about 40 mm, and the width about 1.5 mm. The films were subjected to a statistical tensile strain to place the sample in tension during the sinusoidal axial oscillation, which reached a peak deformation of 0.05%. The complex dynamic modulus was measured by imposing a small dynamic strain to ensure linear viscoelastic behavior of the specimen. The films were annealed for 2 h at 120 °C, prior to the measurements. The measurements were carried out for drawn films with draw ratios <40, since the viscoelastic spectrometer was not sensitive enough to detect small changes of tan δ in films drawn beyond 40.

Results and Discussion

Figures 2 and 3 show the temperature dependence of the apparent crystal lattice modulus of the ($\bar{1}13$) plane. It is evident that within experimental error, the measured values are 43 GPa at temperatures below 155 °C but that the value at 160 °C is 21 GPa, which corresponds to a 50% decrease. Thus it turns out that the real crystal modulus in the chain direction is in the range 40.6–41.4 GPa at temperatures below 155 °C and is in the range 19.8–20.2 GPa at 160 °C, as derived by a somewhat complicated

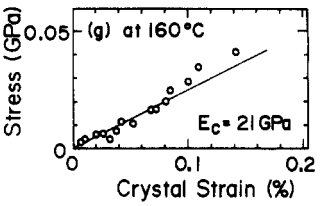

Figure 3. Relationship between the crystal lattice strain of the ($\bar{1}13$) plane and the applied stress at 160 °C for a drawn specimen with a draw ratio of 100.

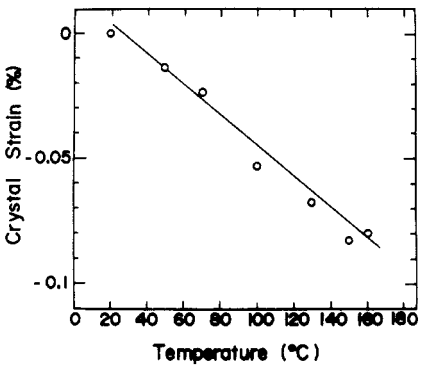

Figure 4. Crystal lattice strain of the ($\bar{1}13$) plane vs temperature at an applied stress of 4.3 MPa.

mathematical treatment of the relationship between the crystal strain of the ($\bar{1}13$) plane and the external applied stress, discussed in the previous paper.[2] At temperatures above 160 °C but below the apparent melting point of the polypropylene films used for differential scanning calorimetry (DSC) measurements,[15] the test specimens were torn at the position where they were irradiated by the X-ray beam at stresses >0.02 GPa. This thermal property of polypropylene films is quite different from that of polyethylene films. For ultradrawn polyethylene films, the crystal lattice modulus is independent of temperature up to 145 °C (close to the equilibrium melting point of 145.5 °C[8]), and the value decreased by only 41% even at 150 °C. The reason for this difference in heat resistance between polyethylene and polypropylene films remains an open question.

Figure 4 shows the thermal expansion behavior of the ($\bar{1}13$) plane at a constant stress of 4.3 MPa. The plots are represented by a straight line up to 160 °C, but the data were scattered beyond 160 °C. The linear thermal expansion coefficient of the ($\bar{1}13$) plane was estimated to be -6.18×10^{-5}/°C from the slope of the line. The linear thermal expansion coefficient in the direction of the c axis can be approximated from that of the ($\bar{1}13$) plane as follows:

$$\alpha'_{33} = \alpha_{33} \cos^2 \phi_3 + (1 - \cos^2 \phi_3)\alpha_{11} \quad (1)$$

where α'_{33}, the linear thermal expansion coefficient of the ($\bar{1}13$) plane, and α_{33} correspond to coefficients parallel and perpendicular to the c axis, respectively. The derivation of eq 1 is shown in the Appendix. From the crystallographic viewpoint, $\cos \phi_3$ in eq 1 is given by

$$\cos \phi_3 = \frac{3ab \sin \beta}{(b^2c^2 + 9a^2b^2 + a^2c^2 \sin^2 \beta + 6ab^2c \cos \beta)^{1/2}} \quad (2)$$

All the coefficients in eq 2 are given by $a = 6.65$ Å, $b = 20.96$ Å, $c = 6.50$ Å, and $\beta = 99.20°$.[18] Substituting all the coefficients into eq 2, we find that $\cos \phi_3 = 0.99068$. In eq 1, α_{11} is an unknown parameter. However, we can neglect the second-order term in eq 1, since $(1 - \cos^2 \phi_3)$

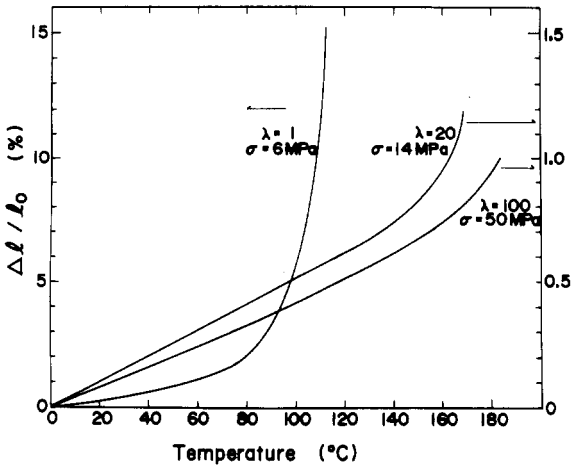

Figure 5. Temperature dependence of bulk strain in the stretching direction for specimens with λ = 1, 20, and 100 at the indicated applied stresses.

is 0.01856. Thus the linear thermal expansion coefficient of the c axis can be estimated to be -6.42×10^{-5}/°C. This value indicates that the shrinkage of the c axis of polypropylene with temperature is higher than that of polyethylene (-2.27×10^{-5}/°C).

Figure 5 shows the thermal expansion behavior of the bulk specimens in the stretching direction as measured at the indicated stresses. The thermal strain of the undrawn specimen increases with increasing temperature, and this tendency is pronounced at temperatures above 80 °C. The thermal strains of the drawn films increase very slightly with increasing temperature up to 150 °C, but the degree of increase becomes somewhat more pronounced beyond 150 °C. The increase in bulk strain with temperature is quite different from the thermal behavior of the crystal lattice strain, as shown in Figure 4. This discrepancy is postulated to be an increase in the amorphous content with increasing temperature.

To test this concept, the temperature dependence of crystallinity was determined by using a drawn film with λ = 100. The crystallinity was estimated from the X-ray diffraction intensity distribution, which was measured at a step interval of 0.1° with a time of 10 s in the range 5–46° (twice the Bragg angle $2\theta_B$) and was represented as a function of Is^2 versus s, in which I is the X-ray diffraction intensity and s is given as $2 \sin \theta/\lambda$ (λ is the wavelength of the X-ray). This operation was carried out for each polar angle in steps of 10° in the range 0–90°. Through this process, the resultant intensity distributions were averaged without using any weighting factor. If $A(T)$ and $A(T_0)$ are the areas of the average diffraction intensity curves at T and T_0 (20 °C), respectively, the crystallinity $X_c(T)$ at T is given by[3]

$$X_c(T) = 86.4A(T)/A(T_0) \quad (3)$$

where 86.4 is the percentage of crystallinity measured by pycnometry at 20 °C.

The decrease in the area of the X-ray diffraction intensity distribution curve for the crystalline phase is attributed to a decrease in crystallinity and an increase in thermal fluctuation caused by lattice distortion. The two contributions were separated by Ruland[19] for undrawn polypropylene films prepared by different methods. Unfortunately, we could not apply his method to the present ultradrawn polypropylene film (λ = 100), since the specimen was torn at the position where it was irradiated by the X-ray beam for several hours at temperatures above 120 °C. In spite of the difficulty in measuring the lattice distortion, it seems that the present treatment is reasonable for estimating the temperature dependence of crystallinity, since the crystal lattice modulus is independent of temperatures up to 145 °C as shown in Figure 2 and 3. It would be expected that if the lattice distortion causes a significant decrease in the area of X-ray diffraction curve, the crystal lattice modulus should decrease with increasing temperature.

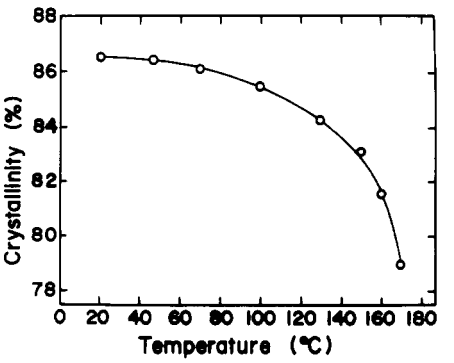

Figure 6. Temperature dependence of crystallinity of a drawn film with λ = 100 at a fixed dimension in the stretching direction.

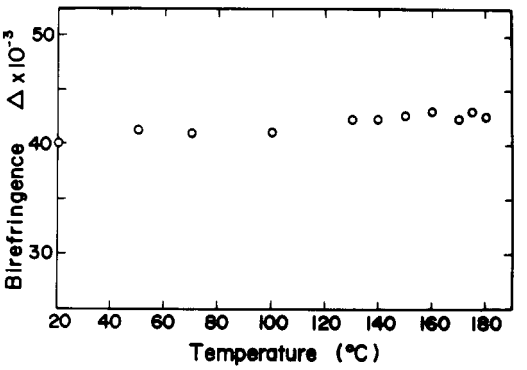

Figure 7. Temperature dependence of birefringence for a drawn film with λ = 100 at a fixed dimension in the stretching direction.

Figure 6 shows the change in crystallinity with increasing temperature at a fixed dimension in the stretching direction. The crystallinity decreases slightly. This tendency is pronounced at temperatures above 140 °C, and the crystallinity at 170 °C becomes 78.5%, a 9.1% decrease. If the lattice distortion were considered in calculating the crystallinity, the temperature dependence of crystallinity would be less.

Figure 7 shows the change in birefringence with increasing temperature. The birefringence is independent of temperature, and the values are in the range (40–43) × 10^{-3}; these values are lower than the intrinsic crystal birefringence (46.2×10^{-3}) and the intrinsic amorphous birefringence (43×10^{-3}) reported by Kuribayashi[20] but are higher than the values of Samuels[21] and Tsvetkov.[22] The form birefringence cannot be neglected because a number of voids were observed within the drawn specimens by scanning electron microscopy.[15] Unfortunately, there is no way at present to estimate the form birefringence in our laboratory. The result in Figure 7 indicates that, even as a crude approximation, the temperature dependence of the molecular orientation cannot be observed from the birefringence in spite of a transition from crystal to amorphous state as shown in Figure 6. This means that birefringence is not sensitive enough to detect small changes in molecular orientation due to the transition.

To facilitate understanding of mechanical properties of bulk specimens in relation to the temperature dependence of the transition and the crystal lattice modulus, the dynamic mechanical properties are discussed in terms of relative molecular orientation. The temperature depen-

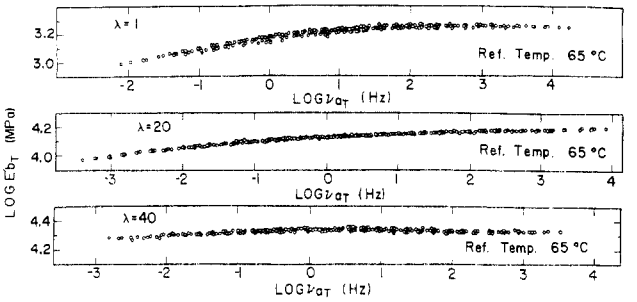

Figure 8. Master curves of the storage modulus E' for drawn specimens with λ = 1, 20, and 40.

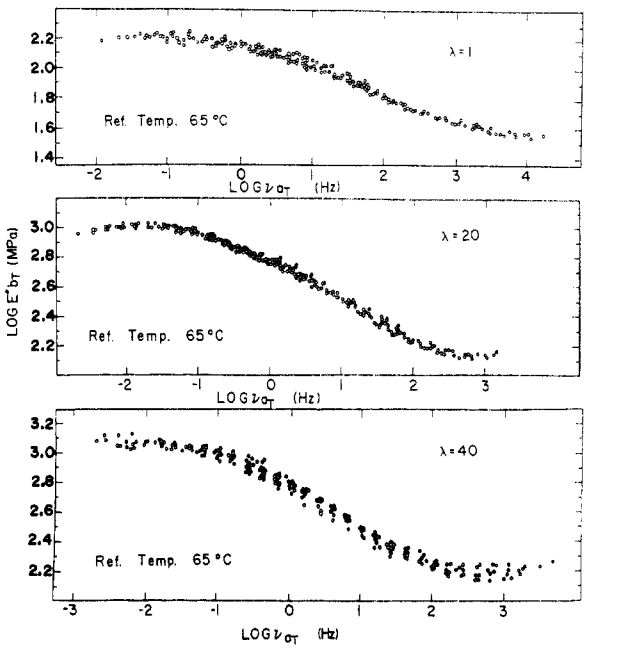

Figure 9. Master curves of the loss modulus E'' for drawn specimens with λ = 1, 20, and 40.

dence of the complex dynamic modulus was measured in the frequency range from 0.1 to 100 Hz for each temperature in step of 10 °C in the range 20–160 °C. Superposition was realized by a combination of horizontal and vertical shifts resulting in apparent master curves of the storage and loss modulus function. Figures 8 and 9 show the master curves of the storage modulus E' and the loss modulus E'', respectively, for the dry gel films with λ = 1, 20, 40, reduced to the common reference temperature of 65 °C. Each curve is obtained by shifting horizontally and then vertically until good superposition is achieved. The profiles of E' show that the frequency dependence becomes smaller with increasing draw ratio. Furthermore it is seen that the frequency dispersion exhibits quite a broad dispersion peak and the profiles are not symmetrical with respect to the logarithmic frequency axis. From these observations, it can be inferred that although the broad dispersion curves may be expected to consist of more than two mechanisms, the direct separation of the reduced modulus into the respective contributions cannot be carried out owing to the lack of adequate data, especially in the lower frequency range. The master curves could not be observed for films drawn beyond λ = 40, because of the scattered values of E'' versus frequency.

To classify the broad dispersion curve into several components, the logarithm of the temperature dependence of the horizontal shift factor $a_T(T,T_0)$ was plotted in logarithmic term versus the reciprocal of the absolute temperature as shown in Figure 10, and the corresponding vertical shift factors $b_T(T,T_0)$ of E' and E'' were plotted

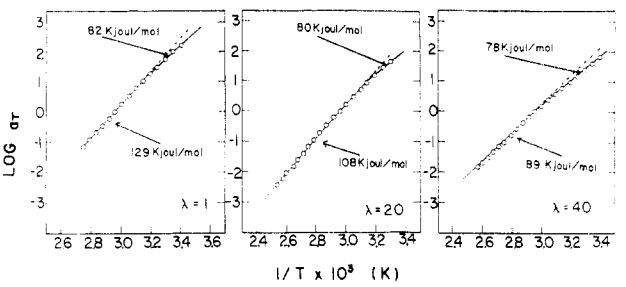

Figure 10. Arrhenius plots of the horizontal shift factors $a_T(T,T_0)$ for drawn specimens with λ = 1, 20, and 40.

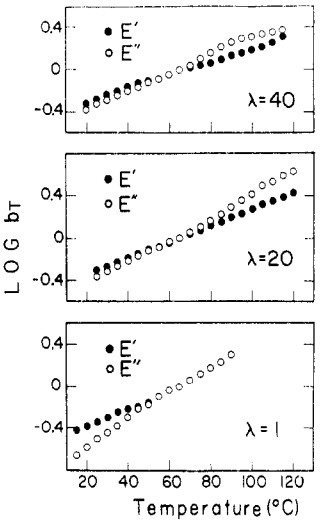

Figure 11. Logarithm of the vertical shift factors $b_T(T,T_0)$ vs temperature for drawn specimens with λ = 1, 20, and 40.

against a linear scale of temperature, as shown in Figure 11. The Arrhenius plots thus obtained in Figure 9 are represented by two straight lines for all the specimens, indicating two relaxation mechanisms. The corresponding temperature regions suggest that the changing slopes manifest the α and β processes. The activation energies of the α and β retardation processes obtained here are in contrast with the small values that have been reported for undrawn films.[23-25] The activation energies of the β and the α processes were reported by Wada to be 167 and 251 kJ/mol, respectively, from dielectric relaxation[23] and to be 155 and 197 kJ/mol from the master curves of the storage and loss compliance functions of a spherulitic sample.[24] Furthermore, activation energies were reported by Onogi et al.[25] on the basis of the master curves of relaxation modulus, using quenched and annealed films whose crystallinities were 50 and 68%, respectively. According to their report,[25] the activation energies of the quenched and annealed films were 211 and 151 kJ/mol, respectively. They concluded that the great difference in activation energy for the α mechanism is to be ascribed to the difference in crystal modification on the basis of the concept that the smectic modification seems to give higher activation energies than the monoclinic form. If their concept is correct, the activation energy of the present undrawn gel film may be a rigorous value, since the crystallinity is higher than that of their annealed sample.

Here it should be noted that no retardation process corresponding to the α_2 mechanism of polyethylene is observed for polypropylene, as has been discussed by Fujita et al.[24] This reason is that the temperature dependence of polypropylene is not appreciable over the range of temperature covered, in contrast with a rather strong dependence for polyethylene at high temperature possibly owing to the activation of the α_2 mechanical retardation

process. The activation energy of the α process decreases considerably with increasing draw ratio, while that of the β process decreases only slightly. The vertical shift factors of E' and E'' become lower as the draw ratio increases.

Returning to Figure 1, it is seen that the c axes of specimens drawn beyond 20 orient to the stretching direction predominantly. Therefore, it would be expected that the α mechanism for films with $\lambda = 20$ and 40 is related to the slippage of crystal grains in the stretching direction, when the applied excitation is parallel to molecular chain axis. If the fractional coefficient between the grains along the chain axis associated with the slippage is lower than that associated with the rotation of the grains within the lamellae owing to the imperfections in the crystal lamellae, the β peak shifts to a lower temperature with increasing draw ratio.[15] This indicates that segmental motions in the amorphous regions become less pronounced, since the crystallinity decreases and the amorphous phase behaves somewhat like paracrystalline. If this is the case, the segmental motions for the films with $\lambda = 20$ and 40 are related to the slippage of amorphous chain segments in the molecular chain axis, and this behavior becomes somewhat elastic. Hence, the activation energy of the β mechanism decreases with increasing draw ratio. This indicates that the activation energy of the α mechanism becomes lower with increasing draw ratio, and the final value will be close to that of the β mechanism for an extremely high molecular orientation, because of a decrease of grain boundary regions. As for an ultradrawn film ($\lambda = 100$), as discussed before, the crystal lattice modulus is not subject to temperature up to 155 °C, and a drastic decrease in crystallinity with temperature is not observed due to high crystallinity and the perfection of the crystal lamellae in addition to the high orientation of the molecules. This suggests that only the β mechanism is observed for an ultradrawn film ($\lambda = 100$) over the range of temperature employed.

Conclusion

From the above considerations, two main conclusions can be drawn.

First, the temperature dependence of the crystal lattice modulus was observed by X-ray diffraction using ultradrawn polypropylene films with draw ratios >80 and was found to be in the range 40.6–41.4 GPa; the values were independent of temperature up to 155 °C. This thermal behavior is quite different from that of bulk specimens. The storage modulus E' decreased with increasing temperature even for ultradrawn films ($\lambda = 100$). The linear thermal expansion coefficient of the c axis was -6.42×10^{-5}/°C. In contrast, the thermal expansion coefficients of bulk specimens in the stretching direction were positive.

Second, the mechanical relaxation of bulk specimens was analyzed in terms of the relative molecular orientation. The temperature dependence of the complex dynamic tensile moduli was measured in the frequency range 0.1–100 Hz for specimens with draw ratios of 1, 20, and 40. The master curves were constructed by shifting horizontally and then vertically. The Arrhenius plots could be represented by two straight lines, indicating the existence of two kinds of relaxation processes. Considering the temperature range covered, it was confirmed that the low- and high-temperature relaxations correspond to the β and α dispersion mechanisms, respectively. The activation energies of both mechanisms decreased with increasing draw ratio. This tendency was pronounced for the α mechanism.

Acknowledgment. We thank Dr. Suehiro, Department of Polymer Chemistry, Faculty of Engineering, Kyoto University, for valuable comments and suggestions to produce an apparatus for measuring the crystal lattice strain by X-ray diffraction.

Appendix

By use of the same geometrical arrangements in Figures 1 and 2 in the previous paper,[2] the component of strain ϵ_{ij} may be given by using the components of linear thermal expansion coefficient α_{ij} and the elastic compliance S_{ij}, as follows:

$$\begin{aligned} \epsilon_{11} &= S_{13}\sigma + \alpha_{11}\Delta T \\ \epsilon_{22} &= S_{23}\sigma + \alpha_{22}\Delta T \\ \epsilon_{33} &= S_{33}\sigma + \alpha_{33}\Delta T \\ \epsilon_{23} &= \epsilon_{13} = \epsilon_{12} = 0 \end{aligned} \tag{A1}$$

where the subscripts 3 and 2 are chosen in the directions of the X_3 and X_2 axes, respectively, and σ is uniform stress along the X_3 axis. ΔT is the difference between the measured temperature and the reference one.

According to the method discussed in the previous paper,[2] the crystal strain ϵ'_{33} of the ($\bar{1}13$) plane may be given by

$$\epsilon'_{33} = \{(\cos^2\phi_3)S_{33} + (1 - \cos^2\phi_3)S_{13}\}\sigma + \{(\cos^2\phi_3)\alpha_{33} + (1 - \cos^2\phi_3)\alpha_{11}\}\Delta T \tag{A2}$$

Equation A2 indicates that the strain ϵ'^{33} can be separated into two components associated with stress and temperature. Thus we have

$$S'_{33} = \epsilon'_{33}/\sigma = (\cos^2\phi_3)S_{33} + (1 - \cos^2\phi_3)S_{13} \tag{A3}$$

$$\alpha'_{33} = \epsilon'_{33}/\Delta T = (\cos^2\phi_3)\alpha_{33} + (1 - \cos^2\phi_3)\alpha_{11} \tag{A4}$$

S'_{33} and α'_{33} correspond to the elastic compliance and the linear thermal expansion coefficient of the ($\bar{1}13$) plane.

Registry No. Polypropylene, 25085-53-4.

References and Notes

(1) Matsuo, M.; Sawatari, C. *Macromolecules* **1986**, *19*, 2036.
(2) Sawatari, C.; Matsuo, M. *Macromolecules* **1986**, *19*, 2653.
(3) Matsuo, M.; Sawatari, C. *Macromolecules* **1988**, *21*, 1653.
(4) Sawatari, C.; Matsuo, M. *Colloid Polym. Sci.* **1985**, *263*, 783.
(5) Matsuo, M.; Sawatari, C. *Macromolecules* **1988**, *21*, 1317.
(6) Smith, P.; Lemstra, P. J. *J. Mater. Sci.* **1980**, *15*, 505.
(7) Smith, P.; Lemstra, P. J. *Colloid Polym. Sci.* **1980**, *258*, 891.
(8) Flory, P. J.; Vrij, A. J. *J. Am. Chem. Soc.* **1963**, *85*, 3548.
(9) Matsuo, M.; Sawatari, C. *Macromolecules* **1988**, *21*, 1658.
(10) Termonia, Y.; Meakin, P.; Smith, P. *Macromolecules* **1985**, *18*, 2246.
(11) Termonia, Y.; meakin, P.; Smith, P. *Macromolecules* **1986**, *19*, 154.
(12) Suehiro, S.; Yamada, Y.; Inagaki, H.; Kyu, T.; Nomura, S.; Kawai, H. *J. Polym. Sci., Polym. Phys. Ed.* **1979**, *17*, 763.
(13) Kawai, H.; Suehiro, S.; Kyu, T.; Shimomura, A. *Polym. Eng. Rev.* **1983**, *3*, 109.
(14) Peguy, A.; Manley, R. S. J. *Polym. Commun.* **1984**, *25*, 39.
(15) Matsuo, M.; Sawatari, C.; Nakano, T. *Polym. J. (Tokyo)* **1986**, *18*, 759.
(16) Roy, S. K.; Kyu, T.; Manley, R. S. J. *Macromolecules* **1988**, *21*, 499.
(17) Matsuo, M.; Manley, R. S. J. *Macromolecules* **1983**, *16*, 1500.
(18) Natta, G.; Corradini, P. *Nuovo Cimento* **1956**, *15* (Ser. 10), 40.
(19) Ruland, W. *Acta Crystallogr.* **1961**, *14*, 1180.
(20) Kuribayashi, S.; Nakai, A. *Seni-Gakkaishi* **1962**, *3*, 1741.
(21) Samuels, R. J. *J. Polym. Sci., Part A-2* **1965**, *3*, 1741.
(22) Tsvetkov, V. N. *Newer Method of Polymer Characterization*; Interscience Publishers: New York, 1964; p 563.
(23) Wada, Y. *J. Phys. Soc. (Jpn.)* **1961**, *16*, 1226.
(24) Fujita, K.; Daio, M.; Okumura, R.; Suehiro, S.; Kawai, H. *Polym. J. (Tokyo)* **1983**, *15*, 449.
(25) Onogi, S.; Fukui, Y.; Asada, T.; Naganuma, Y. *Proc. Int. Congr. Rheol., 5th* **1970**, *4*, 87.